www.cadanda.com
Computer-Aided Design AND APPLICATIONS

Optimum Design of Diamond Saw Blades Based on Experimentally Verified Finite Element Models

Kun-Nan Chen[13], Chu Chang[1] and Jing-Chung Huang[2]

[1]Department of Mechanical Engineering, Tungnan University, Taipei, Taiwan
[2]Department of Mechatronic Technology, Tungnan University, Taipei, Taiwan
[3]Corresponding author, knchen@mail.tnu.edu.tw

ABSTRACT

This paper proposes a two-phased procedure for the optimum design of circular diamond saw blades. In Phase one, an accurate finite element (FE) model representing an actual saw blade is acquired by incorporating experimental and finite element analysis (FEA) frequencies to update the blade FE model. In Phase two, shape optimization of the radial slots on the blade, based on the updated geometrical parameters obtained in Phase one, is performed to maximize the frequency separation between the FEA results and the saw's operational speed, in an attempt to reduce the possibility of structural resonance. The effectiveness of the proposed two-phased system is demonstrated by the successful implementation of several numerical examples.

Keywords: optimum design, finite element model updating, saw blades, modal testing.
DOI: 10.3722/cadaps.2012.571-583

1 INTRODUCTION

Circular diamond saws, which work in high speed, are widely used to cut, dice or groove materials such as rock, metal, ceramics, optical glasses and electronic materials with high machining efficiency. For the electronics industry, the advantage of using diamond saws is that they can cut efficiently high aspect ratio work-pieces that are made of single-crystal structure or contain rare-earth elements, which are normally difficult to cut with other means and are generally very expensive. The machining speed of diamond saws for cutting Si wafers of thickness 200 μm can be more than three times as fast as that of UV lasers [1]. For wafers greater than 1 mm in thickness, abrasive diamond saws are the only logical choice for cutting.

Figure 1(a) shows a common circular diamond saw blade. The main body of the saw blade is usually made of carbon steel or manganese steel, e.g. 65Mn steel. The blade tip is slightly thicker than

the blade body and diamond grits of sizes in micro meters are adhered to the blade tip by the cataphoresis process. Some diamond saw blades have radial or/and annular slots symmetrically distributed about the center hole. These narrow slots are used to increase the thermal dispersion efficiency of the blade and to reduce vibration and noise when the blade rotates in high speed. Several commercially available circular diamond saw blades can be seen in Fig. 1(b).

During a cutting process, a saw blade can produce a high level of noise and even cause severe noise pollution in the work place. There are three different sources of noise created by a running blade: resonant, aerodynamic and mechanical noise. When the rotation speed is at or near one of the natural frequencies of the blade, resonance occurs and vibration and noise levels increase dramatically. Cho and Mote [2] concluded that a rotating blade causes the surrounding air molecules to vibrate violently, generating fluctuating air pressure, and hence produces aerodynamic noise. Mechanical noise is usually formed by friction and impact between the blade tips and work piece. An idling blade rotating in high speed may generate **ò**whistling noise,**ó** one form of resonant noise. Increasing the damping of the blade can effectively reduce the possibility of whistling noise occurrence. Hattori and Iida [3] experimented on blades made of high-damping alloy and successfully suppressed the level of whistling noise. Slots or openings on a blade may weaken the blade structure but also decrease the vibration and noise intensity. Singh [4], through experimentation, observed the effects of radial slots on idling blades and found that radial openings destroyed the continuity of vibrational mode shapes of the blades, and sound wave transmission was also obstructed due to geometrical discontinuity. As a result, both vibration and noise levels were significantly diminished. Other research works about circular saw blades include: Ishihara *et al.* [5] studied the dynamic behavior of thermally loaded circular disks based on plate bending theories; and Schajer and Steinzig [6] employed Electronic Speckle Pattern Interferometry (ESPI) to measure the natural frequencies and mode shapes of saw blades.

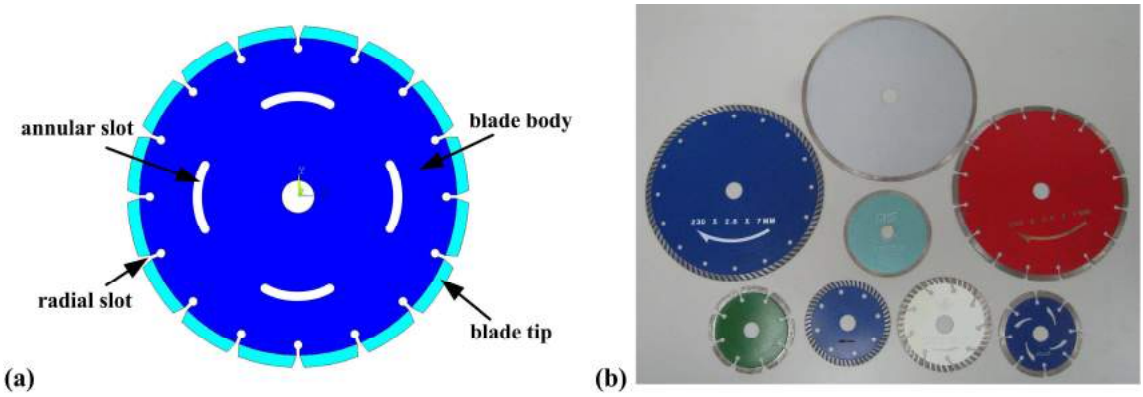

Fig. 1: (a) Circular diamond saw blade, and (b) some commercial saw blades.

To study the dynamic behavior of a diamond saw blade, both experimental techniques and the finite element method (FEM) may be employed. Applying FEM to analyze a structure requires the geometrical and material properties of the structure as input parameters. A small error in one input parameter can produce large deviations from the true structural responses. In order to obtain a more accurate and reliable finite element (FE) model of a structure, the FE model updating (or tuning) has been an active research area [7-10]. Usually combined with an optimization technique, an FE model

updating procedure modifies the FE model and seeks to minimize the difference between the analysis and the experimental results. The updated FE model is considered to be a better model for future dynamic response predictions or design modifications. Arora *et al.* [11] proposed a two stage updating procedure, in which the mass and stiffness matrices are first updated, and then the damping matrix whose effects are normally excluded in the updating process. When applying the model updating procedure, a better result may be obtained if the resolution (degrees of freedom) of the experimentally measured data can be enhanced. Wang *et al.* [12] utilized a high-speed digital camera and an image processing technique to acquire a massive amount of full-field mode shape data for model updating. The updating concept can also be applied to other areas. Fang and Perera [13] applied the tuning technique to structural damage detection problems. In a tutorial presentation, Mottershead *et al.* [14] discussed several simple examples and a large scale example of a helicopter airframe using a sensitivity-based updating procedure.

This paper presents a two-phased procedure for the shape optimization of circular diamond saw blades. In the first phase the FE model updating concept is utilized to create an FE model accurately representing a practical saw blade; then in the second phase, based on the updated FE model, the shape optimization for the blade is performed according to various criteria. The optimization results should provide improved designs for saw blades that produce minimal vibration and noise during operation. The finite element analysis (FEA) and the shape optimization are carried out by the use of the commercial software ANSYS, which employs a forward difference scheme to approximate the required derivatives and gradient vectors.

2 OPTIMUM DESIGN BASED ON FINITE ELEMENT UPDATED MODELS

A flowchart for the optimum shape design of circular diamond saw blades using the proposed two-phased optimization procedure can be seen in Fig. 2. The rationale behind this two-phased procedure is that not only the final optimum designs, derived from the updated model of the initial design, are feasible but also saw blades based on the optimum designs can be manufactured under a similar condition as for the original blades. This is valuable since alterations of the original design to the optimum shapes are likely to incur no extra cost to the manufacturer.

2.1 Phase One: Finite Element Model Updating

At this phase, an optimization problem is formed by combining two sets of natural frequencies and mode shapes of the same structure, one from a modal test and the other from a finite element analysis, and then the problem is solved to give a set of updated geometrical parameters. The process begins with measurements of the natural frequencies and mode shapes of the structure tested. The finite element model of the structure is created and then analyzed. Since the values of the finite element input parameters are often not precise, it is very likely that the measured and the predicted results will show a significant discrepancy. By carefully comparing the experimental and FEA mode shapes, matching modes are correctly paired, which is important since the order of the FEA modal data can be different from that of the measured data. By defining the error vector as a vector containing the relative differences between the experimental and FEA natural frequencies, an optimization problem can be formulated as to minimize the length of the error vector as follows:

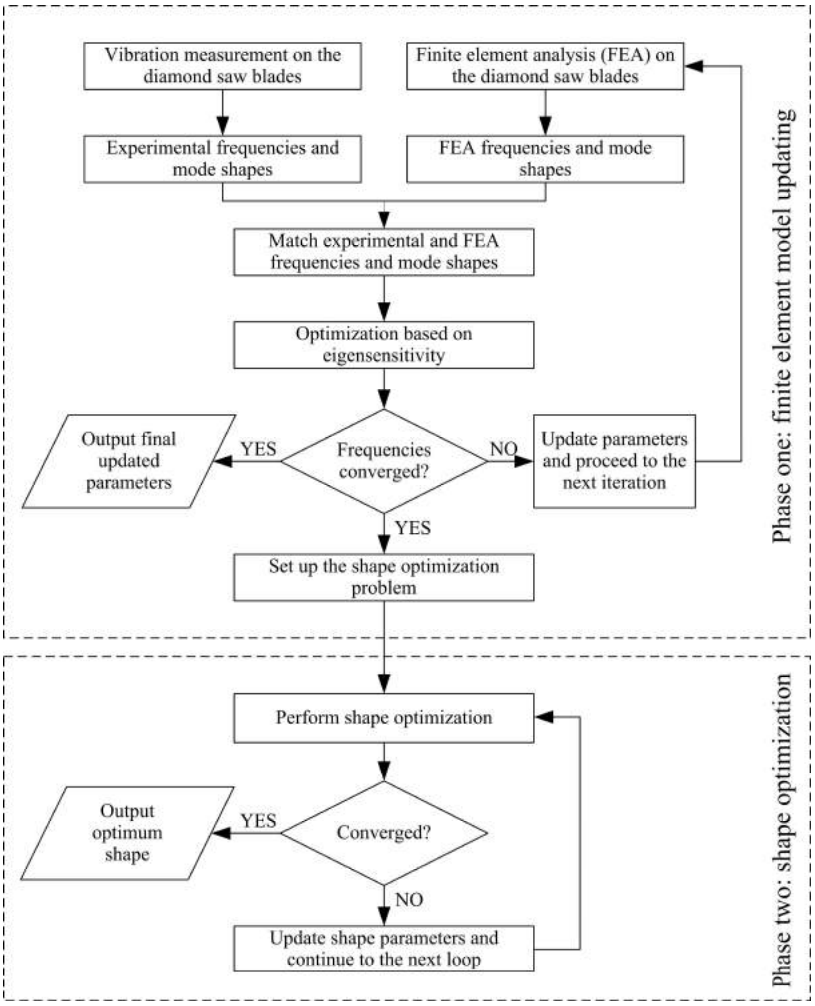

Fig. 2: Flowchart for the two-phased shape optimization procedure.

$$Minimize \quad \|e\| = \left[\sum_{i=1}^{m} e_i^2\right]^{\frac{1}{2}} \tag{2.1}$$

$$Subject\ to \quad e_i = \frac{f_i^a - f_i^e}{f_i^e} \qquad i = 1,\ldots,m \tag{2.2}$$

$$\left|m_T - M\right| \le \varepsilon \tag{2.3}$$

$$X_{jL} \le x_j \le X_{jU} \qquad j = 1,\ldots,n \tag{2.4}$$

where f_i is the natural frequency for the matched mode i; the superscripts a and e represent FEA and experimental results, respectively; m_T represents the total mass of the blade FE model, M the measured mass and ε a small positive value; F_{iL} and F_{iU} are the upper and lower limits for the FEA frequency f_i^a; x_j is the j^{th} FE input parameter considered and X_{jU} and X_{jL} denote its upper and lower

bounds, respectively; m is the number of modes included in the optimization process; and n is the number of FE input parameters to be updated (updating parameters). The number of updating parameters should be kept small and only the uncertain ones should be selected as the updating parameters. In general it is required that $n \leq m$ to ensure a physically meaningful result. This optimization problem is solved to yield a set of updated parameters, and then the results are checked for convergence. If converged, the process can be stopped; otherwise, FEA is once again performed using the updated parameters to produce a new set of modal data leading to the next iteration, and the procedure is continued in an iterative way. To perform optimization, eigensensitivities with respect to changes in the updating parameters are calculated to direct the optimization path.

The thickness of a blade tip is greater than that of blade body to ensure only the tips are in contact with the work piece during cutting as shown in Fig. 3(a). Since the tips are embedded with diamond grids, the tips have very rough surfaces. And the blade body is usually coated with a thick layer of paint, which makes the exact thickness of the blade body difficult to measure. Also it was noted that a slight variation in either the tip or body thickness will cause a significant change in frequencies. Therefore, in this study, the tip thickness, denoted as x_1, and the blade thickness, defined as x_2, were set as the updating parameters. In addition, to reduce the risk of introducing further modeling errors while applying boundary conditions, the modal testing experiment of the blade was conducted under a free-free boundary condition, and so was the finite element model constructed. Figure 3(b) shows the FE grid of the blade as well as the boundary condition.

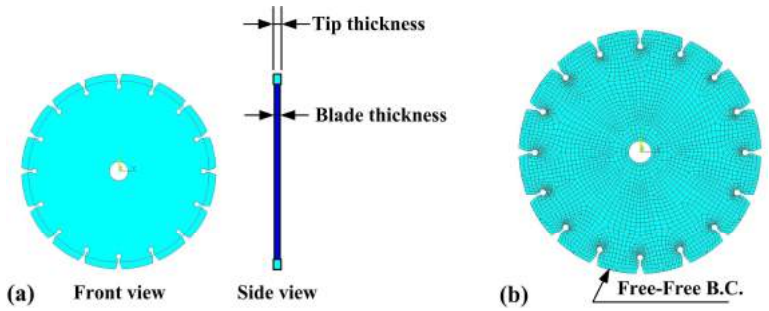

Fig. 3: (a) The blade's front and side views, (b) the FE grid and the boundary condition.

2.2 Phase Two: Shape Optimization

In this phase, the size of the radial slots of a saw blade is optimized by maximizing the frequency differences between the blade's natural frequencies and the saw's operational speed, using the updated model obtained in Phase one as the initial model. The shape optimization problem is formulated as follows:

$$Maximize \quad \left[\sum_{i=1}^{r}\left(f_i^a - \Omega\right)^2\right]^{\frac{1}{2}} \tag{2.5}$$

$$Subject\ to \quad \mathrm{X}_{j\mathrm{L}} \leq x_j \leq \mathrm{X}_{j\mathrm{U}} \qquad j = 1,\ldots,s \tag{2.6}$$

where f_i^a is the same as that defined in Phase one and Ω is the saw's operational rotation speed; x_j in this phase represents the sizing parameters of the radial slots; and r and s represent the number of frequencies and design parameters included in the optimization process, respectively. To maximize the objective function defined in Eqn. (2.5) is to enforce the blade's natural frequencies to separate

from the saw's operational speed as far as possible. Therefore, the possibility of resonance can be minimized. Figure 4(a) shows the parameters defining the size of a radial slot, in which the slot length, slot width and opening angle are denoted as x_1, x_2 and x_3, respectively. The diameter of the circular hole at the end of each slot is set to be proportional to the slot width; hence it is excluded from the design parameters. Before a cutting operation, the saw blade has to be mounted on a sawing machine by clamping the blade with two flanges as shown in Fig. 4(b). The clamping of the blade can be simulated by a fixed boundary condition on the circumference of the flange. Figure 4(c) illustrates the FE grid and this boundary condition.

Both optimization problems in Phases one and two are solved and the FEA are performed using the ANSYS Parametric Design Language (APDL) with the first order optimization scheme. When the first order optimization method is executed, the constrained optimization problem is transformed into an unconstrained one via penalty functions and derivatives are approximated using a forward difference approach.

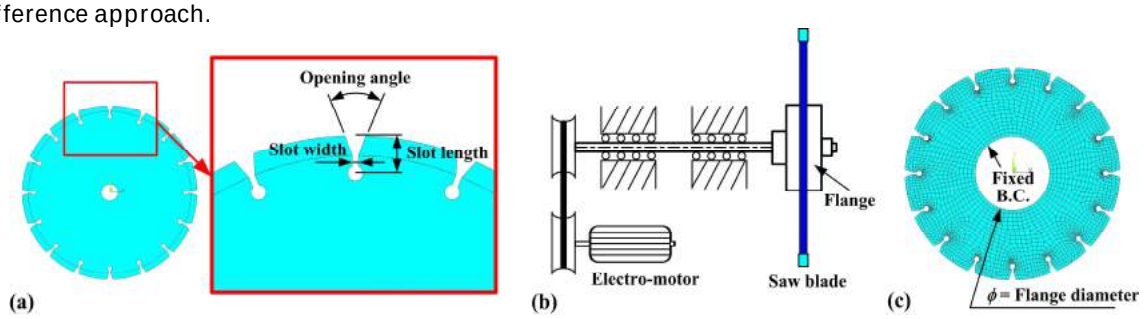

Fig. 4: (a) Parameters defining the size of a radial slot, (b) clamping of the blade in a sawing machine, and (c) the FE grid and the boundary condition.

3 RESULTS AND DISCUSSION

3.1 The Initial Blade Model

A circular diamond saw blade, which has a center hole diameter of 22 mm, an outer diameter of 230 mm and 16 radial slots (slot length: 15 mm, slot width: 2.5 mm and opening angle: 40°), was chosen as the subject to demonstrate the two-phased optimum design procedure. Figure 5 shows the blade in a modal testing experiment setup. The blade body and tip were measured to have thicknesses of roughly 2 mm and 2.6 mm, respectively. A finite element model for the blade in a free-free boundary condition was created using the ANSYS software with SHELL93 elements. Figure 6 displays the FEA frequencies and mode shapes of this initial model, in which Mode (0,2), for example, symbolizes a mode with 0 nodal circle line and 2 nodal diameter lines. Note that due to structural symmetry all modes appear in pairs (orthogonal pairs) except Mode (0,0) (another Mode (1,2) is not shown here). Varying the slot size will cause the natural frequencies to change. Figure 7 shows the effects of slot width and length on the natural frequencies of the blade with the mode number corresponding to its frequency's numerical order. Generally speaking, increasing either the width or the length decreases all frequencies, yet some drops faster than others. When a saw blade revolves, rotation stiffening effects will take place. Faster the blade rotates, higher the frequencies increase. Figure 8 illustrates the blade stiffening result, as functions of the rotation speed, of a blade clamped by flanges of 80 mm in diameter, and the frequencies and mode shapes of a blade rotating at 12000 rpm can be seen in Fig. 9.

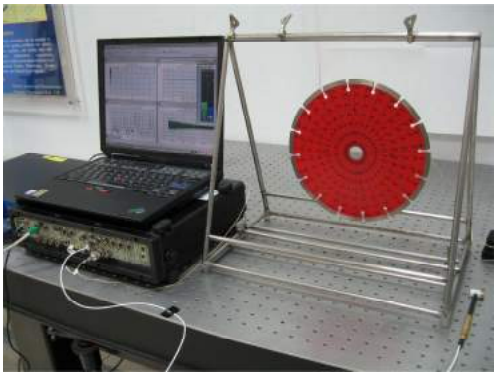

Fig. 5: The saw blade under study in a modal test setup.

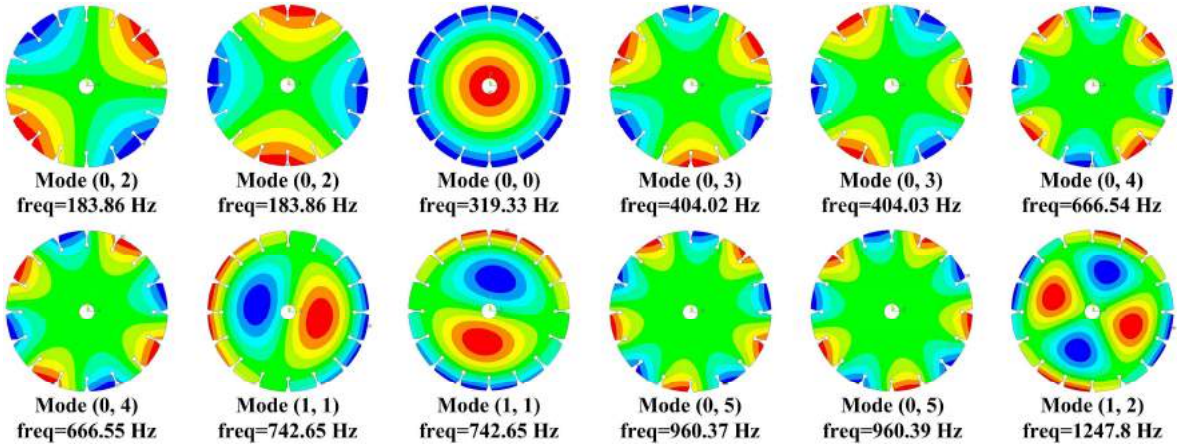

Fig. 6: FEA frequencies and mode shapes of the initial model.

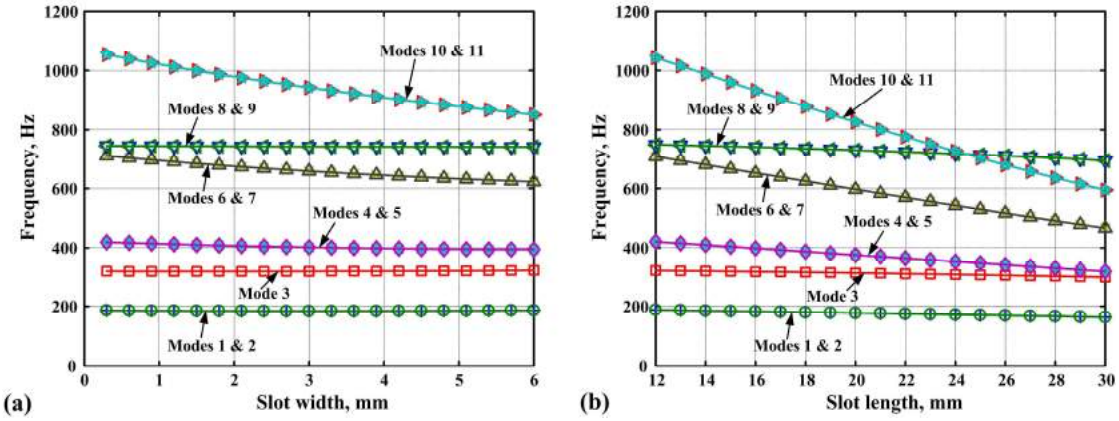

Fig. 7: (a) Effects of slot width and (b) slot length on the natural frequencies.

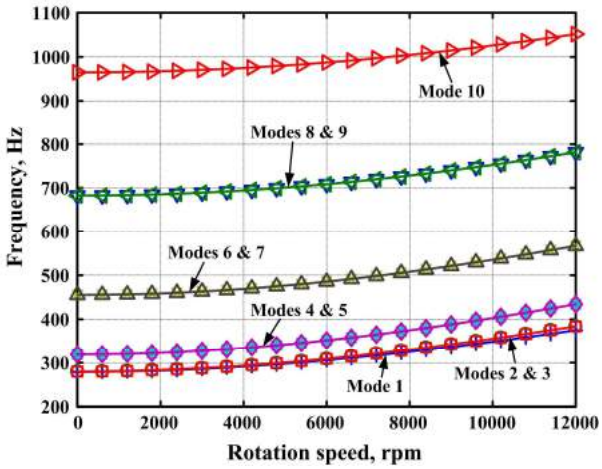

Fig. 8: Stiffening effects as the clamped blade rotates.

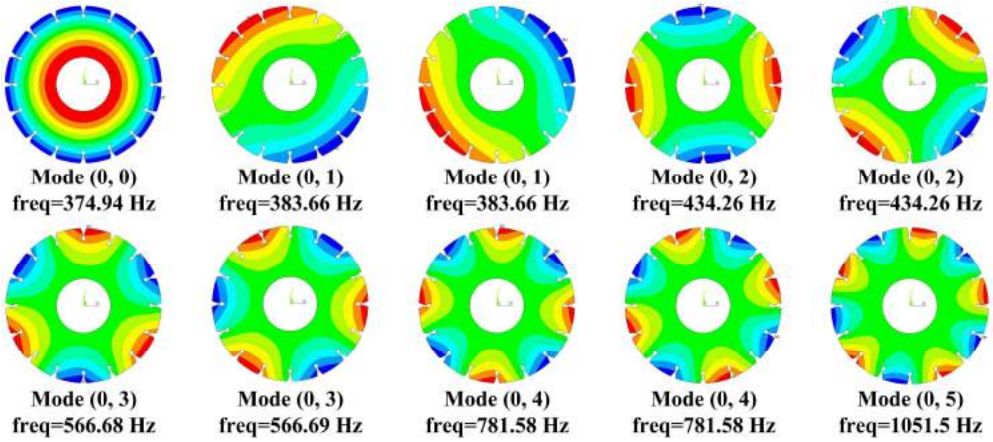

Fig. 9: Natural frequencies and mode shapes of the blade rotating at 12000 rpm.

3.2 Results of Finite Element Model Updating

Before the finite element model updating procedure, the Phase one, can be conducted, modal testing on the blade must be performed and experimental data extracted. The test setup, in which the blade was suspended by two thin strings to simulate a free-free boundary condition and a miniature instrumented impact hammer and a miniature accelerometer were used, can be seen in Fig. 5. Figure 10 shows the bladeís test grid and test results including test frequencies and damping values. Also, the actual blade was measured to have a mass of 531 grams, a value that can be incorporated into the constraint equation for the total mass of the FE model in Eqn. (2.3).

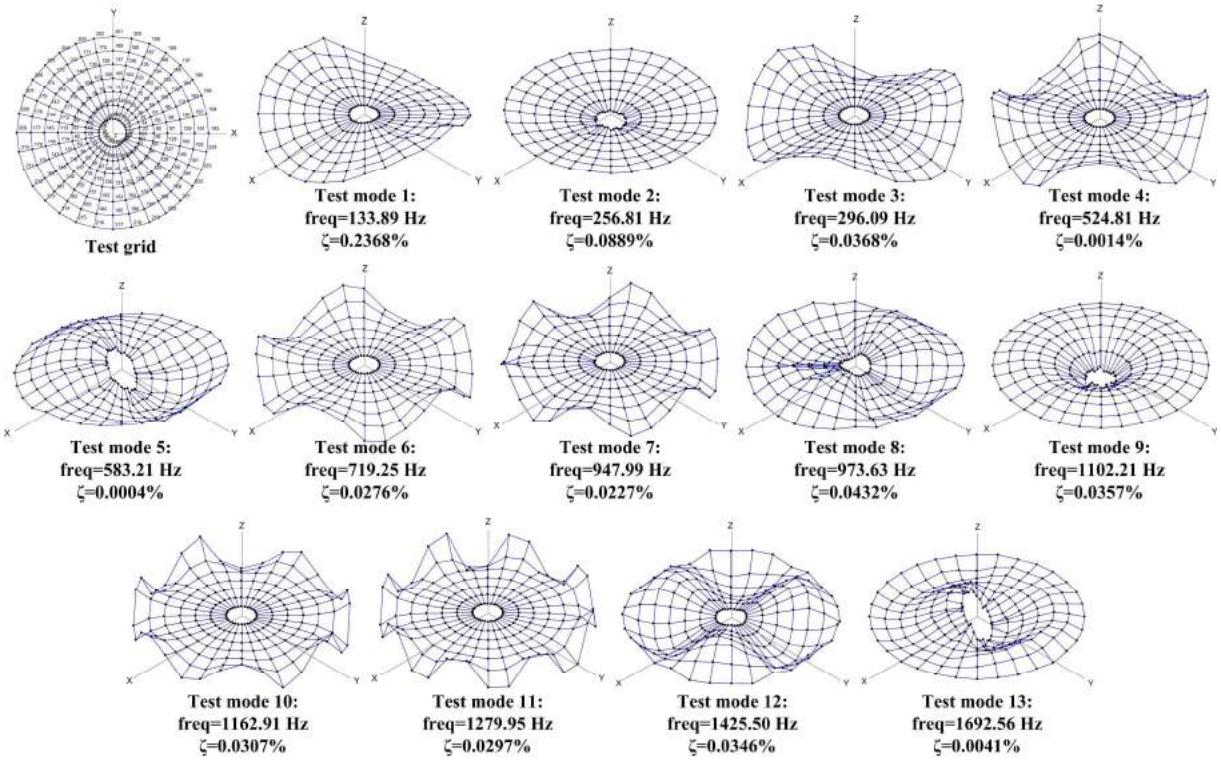

Fig. 10: Test grid and test results of the blade in free-free boundary condition.

Applying the updating scheme of Eqns. (2.1) through (2.4) with m=4, M=531 grams, ε=2 grams and n=2 (x_1: tip thickness and x_2: blade thickness), the updating process converged in 30 iterations. The final updated tip and blade thicknesses are 1.57 mm and 0.97 mm, respectively. Figure 11 shows the iteration histories for the updating parameters x_1 and x_2, the difference between measured and calculated masses, and the objective function (the length of the error vector). A comparison of the FEA and the test frequencies together with their differences before and after the updating procedure are given in Tab. 1. There were significant discrepancies between the test and the initial model's FEA frequencies. The updating technique reduced the disagreements dramatically, from more than 37% the most to less than 5%. Note that in Tab. 1, test modes 5 and 6 were not included in the updating plan (m=4), but the matched FEA modes of the updated model are still in very good agreement with their test counterparts, which may be served as an indicator about how well the updating results are.

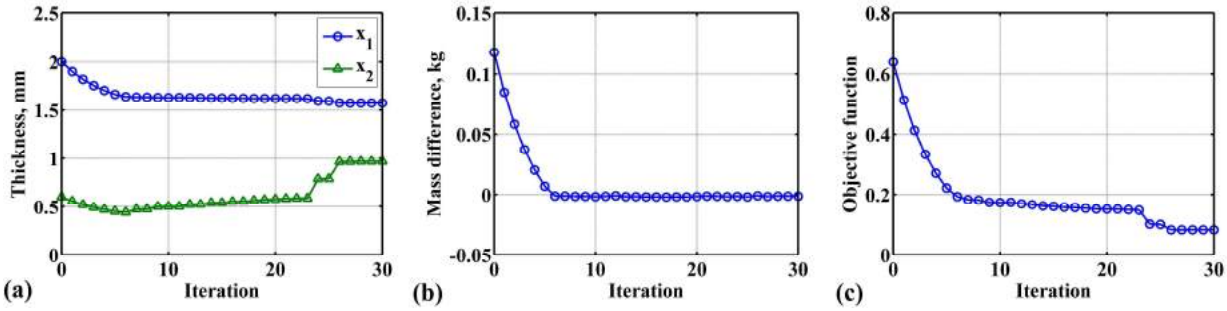

Fig. 11: Iteration histories for (a) updating parameters x_1 and x_2, (b) difference between measured and calculated masses, and (c) the objective function.

Test mode no.	Test frequency (Hz)	Matched FEA mode no.	FEA freq. (Hz) (Initial model)	Freq. difference (%) (Initial model)	FEA freq. (Hz) (Updated model)	Freq. difference (%) (Updated model)
1	133.89	1, 2	183.86	37.32	139.82	4.42
2	256.81	3	319.33	24.34	244.72	-4.71
3	296.09	4, 5	404.02	36.45	306.52	3.52
4	524.81	6, 7	666.54	27.01	505.10	-3.75
5*	583.21	8, 9	742.65	27.34	571.62	-1.98
6*	719.25	10, 11	960.38	33.53	712.33	-0.96

* Test modes 5 and 6 not included for updating

Tab. 1: Comparison of the FEA and the test frequencies together with their differences before and after the updating procedure.

3.3 Results of Shape Optimization

Based on the updated geometrical parameters obtained in Phase one, the blade model was clamped by a pair of flanges of 40 mm in diameter and then analyzed and the slot sizes optimized for two different cases, using Eqns (2.5) and (2.6). Case one is the same blade as the original, which has 16 radial slots, rotated at 24000 rpm or 400 Hz; Case two has 11 slots and is spun at 3000 rpm or 50 Hz. For both cases, the design variables are the three parameters (s=3) characterizing the shape of a radial slot, i.e. x_1: slot length, x_2: slot width and x_3: opening angle, and that two frequency modes (r=2) are included for optimization should be enough to prevent resonance from occurring.

3.3.1 Case one: 16 radial slots, rotated at 24000 rpm

After 33 iterations, the optimization process has converged, and the initial and optimal values of the design variables and the objective function are given in Tab. 2. Also shown in Tab. 2 are the frequency differences for Mode (0,0) (FEA mode no. 1) and Mode (0,1) (FEA mode no. 2 and 3) before and after the optimization. The frequency separation for Mode (0,0) shows a significant improvement from minus 0.669% to 5.819%, which greatly reduces the risk of resonance. Figure 12 illustrates the iteration histories for the design parameters and the objective function, whilst Fig. 13 exemplifies the frequencies and mode shapes of the optimized blade for this case.

Status	Design variables	Frequency separation (from 400 Hz)	Obj. function

	x_1 (mm)	x_2 (mm)	x_3 (°)	Mode (0,0) (%)	Mode (0,1) (%)	f
Initial value	15.00	2.50	40.00	-0.669	14.008	0.140
Optimal value	29.99	4.15	49.64	5.819	15.554	0.166

Tab. 2: Initial and optimal values of the design variables and objective function for Case one.

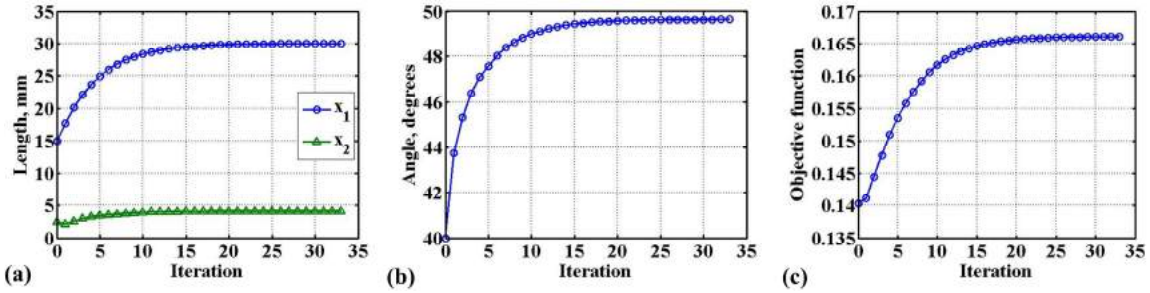

Fig. 12: Iteration histories for Case one: (a) design parameters x_1 and x_2, (b) design parameters x_3, and (c) the objective function.

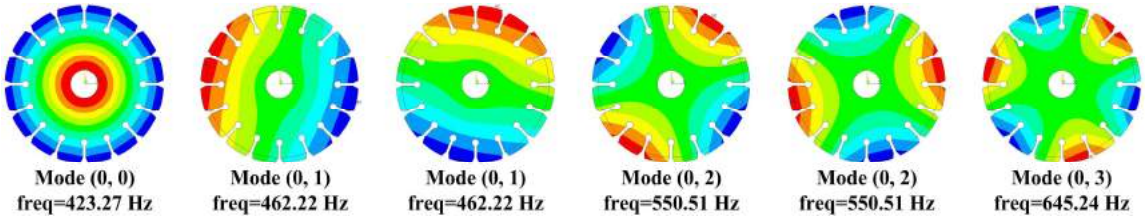

Fig. 13: Natural frequencies and mode shapes of the optimized blade for Case one.

3.3.2 Case two: 11 radial slots, rotated at 3000 rpm

The optimization process of Case two had a hard time to converge. Nevertheless, after 70 iterations, the optimization process has also converged. The initial and optimal values of the design variables and the objective function are given in Tab. 3. In this case, the frequency separation for the initial value of the first mode, Mode (0,1), is large enough so the improvement is not significant. Figure 14 shows the iteration histories for the design parameters and the objective function, whereas Fig. 15 displays the frequencies and mode shapes of the optimized blade for Case two.

Status	Design variables			Frequency separation (from 50 Hz)		Obj. function
	x_1 (mm)	x_2 (mm)	x_3 (°)	Mode(0,1) (%)	Mode(0,0) (%)	f
Initial value	15.00	2.50	40.00	170.270	187.928	2.536
Optimal value	13.79	3.39	52.44	172.798	190.396	2.570

Tab. 3: Initial and optimal values of the design variables and objective function for Case two.

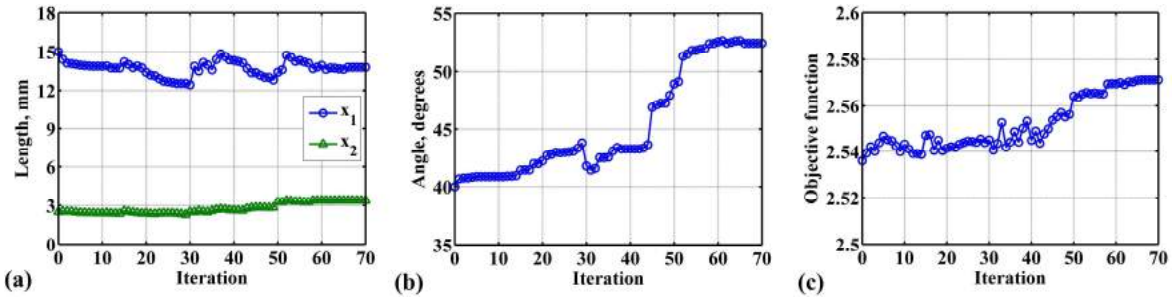

Fig. 14: Iteration histories for Case two: (a) design parameters x_1 and x_2, (b) design parameters x_3, and (c) the objective function.

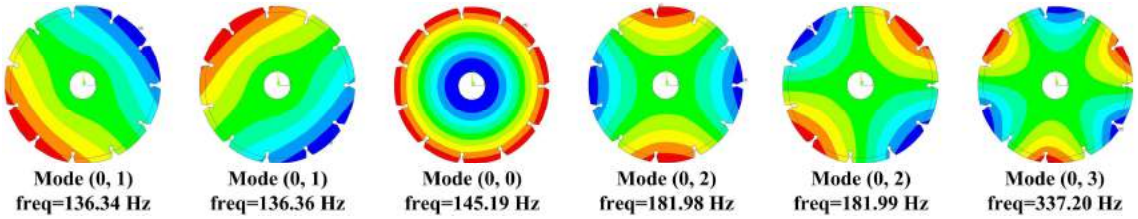

Fig. 15: Natural frequencies and mode shapes of the optimized blade for Case two.

4 CONCLUSIONS

In the present paper, optimum design of circular diamond saw blades using a two-phased procedure has been described. In the first phase, an accurate FE model representing an actual saw blade is acquired by incorporating measured and FEA frequencies to update the blade FE model. In Phase two, shape optimization of the radial slots on the blade, based on the updated geometrical parameters obtained in Phase one, is performed to maximize the frequency separation between the FEA results and the saw's operational speed, in an attempt to reduce the possibility of structural resonance. The optimized saw blades can be manufactured under similar conditions as used for the original blade. Numerical results have demonstrated that in Phase one, the FEA frequencies of the updated model are in excellent agreement with the experimental data. And in Phase two, FEA frequency separation from rotating speed of 50 Hz and 400 Hz has been improved, especially for Case one, in which a considerable raise of frequency separation from -0.669% to 5.819% has been achieved. Overall, the effectiveness of the proposed two-phased system has been verified by the successful implementation of the numerical examples.

REFERENCES

[1] Mizuno, M.; Iyama, T.; Zhang, B.: Analysis of the Sawing Process with Abrasive Circular Saw, Journal of Manufacturing Science and Engineering, 130(1), 2008, Paper no. 011012, 1-15. doi:10.1115/1.2783220

[2] Cho, H. S.; Mote, C. D.: On the Aerodynamic Noise Source in Circular Saws, Journal of Vibration and Acoustics, 44(4), 1979, 662-671.

[3] Hattori, N.; Iida, T.: Idling Noise from Circular Saws Made of Metals with Different Damping Capacities, Journal of Wood Science, 45, 1999, 392-395. doi:10.1007/BF01177911

[4] Singh, R.: Case History: The Effect of Radial Slots on the Noise of Idling Circular Saws, Noise Control Engineering Journal, 31(3), 1988, 167-172. doi:10.3397/1.2827720

[5] Ishihara, M.; Ootao, Y.; Noda, N.: Analysis of Dynamic Characteristics of a Rotating, Thermally Loaded Circular Saw Subjected to Tensioning over a Double Annular Domain, Journal of Solid Mechanics and Materials Engineering, 4(8), 2010, 1155-1166. doi:10.1299/jmmp.4.1155

[6] Schajer, G. S.; Steinzig, M.: Sawblade Vibration Mode Shape Measurement Using ESPI, Journal of Testing and Evaluation, 36(3), 2008, 259-263.

[7] Gant, F.; Rouch, Ph.; Louf, F.; Champaney, L.: Definition and Updating of Simplified Models of Joint Stiffness, International Journal of Solids and Structures, 48(5), 2011, 775-784. doi:10.1016/j.ijsolstr.2010.11.011

[8] Zapico-Valle, J. L.; Alonso-Camblor, R.; Gonzalez-Martinez, M. P.; Garcia-Dieguez, M.: A New Method for Finite Element Model Updating in Structural Dynamics, Mechanical Systems and Signal Processing, 24, 2010, 2137-2159. doi:10.1016/j.ymssp.2010.03.011

[9] Chen, K.-N.: Model updating and optimum designs for V-shaped AFM probes, Engineering Optimization, 38(7), 2006, 755-770. doi:10.1080/03052150600704534

[10] Chen, K.-N.; Gau, W.-H.; Hu, Y.-C.:, Identification of Material and Geometrical Parameters for Microstructures by Dynamic Finite Element Model Updating, Microsystem Technologies, 12(8), 2006, 736-745. doi:10.1007/s00542-006-0110-6

[11] Arora, V.; Singh, S. P.; Kundra, T. K.: Finite Element Model Updating with Damping Identification, Journal of Sound and Vibration, 3248, 2009, 1111-1123. doi:10.1016/j.jsv.2009.02.048

[12] Wang, W.; Mottershead, J. E.; Ihle, A.; Siebert, T.; Schubach, H. R.: Finite Element Model Updating From Full-field Vibration Measurement Using Digital Image Correlation, Journal of Sound and Vibration, 330(8), 2011, 1599-1620. doi:10.1016/j.jsv.2010.10.036

[13] Fang, S. E.; Perera, R.: Damage Identification by Response Surface Based Model Updating Using D-optimal Design, Mechanical Systems and Signal Processing, 25, 2011, 717-733. doi:10.1016/j.ymssp.2010.07.007

[14] Mottershead, J. E.; Link, M.; Friswell, M. I.: The Sensitivity Method in Finite Element Model Updating: a Tutorial, Mechanical Systems and Signal Processing, in press. doi:10.1016/j.ymssp.2010.10.012